J Low Temp Phys (2007) 148: 323–330
DOI 10.1007/s10909-007-9391-0

Pairing, Phase Separation, and Deformation in the BEC-BCS Crossover

G.B. Partridge · Wenhui Li · Y.A. Liao · R.G. Hulet

Published online: 26 May 2007

Abstract We prepare a two-component gas of ^{6}Li atoms which pair at sufficiently low temperatures. The BEC-BCS crossover is realized by tuning the atomic interactions via a broad Feshbach resonance. We determine the closed-channel molecular component of the pairs as a function of interaction strength by measuring the rate of photoexcitation to a molecular state. The molecular component is sufficiently small that the order parameter of the paired superfluid agrees well with a single-channel model of the crossover. We have also produced a gas with unequal numbers of the two spin components. We observe that this polarized gas phase separates into a paired central core, with the excess unpaired atoms residing outside the core. Remarkably, the real-space distributions deform significantly with increasing polarization.

PACS 03.75.Ss · 03.75.Hh · 05.70.Fh · 33.80.Ps

1 Introduction

Fermion pairing is the underlying mechanism for superconductivity in certain solids as well as for superfluidity of ^{3}He. Recently, several groups have explored *s*-wave fermion pairing using ultracold atomic gases with two spin components [1–7]. Experiments with cold atoms are notable because of the ability to tune system parameters with relative ease. For example, the crossover from a BCS superfluid with large Cooper pairs to the regime of Bose-Einstein condensation (BEC) of molecules can be explored by use of a magnetically-tuned collisional (Feshbach) resonance [8]. While the BEC and BCS regimes are well-understood theoretically, a not-so-well understood, but scientifically important strongly interacting regime lies between them.

G.B. Partridge · W. Li · Y.A. Liao · R.G. Hulet (✉)
Department of Physics and Astronomy and Rice Quantum Institute, Rice University, Houston, TX 77005, USA
e-mail: randy@rice.edu

In addition to interaction strength, it is also possible to vary the relative population of the two spin components. Theorists have long speculated about the phases of matter possible with unequal Fermi energies [9]. Exotic phenomena and new ordering may be observable under these conditions, including the Fulde-Ferrell-Larkin-Ovchinnikov (FFLO) state [10, 11], in which the pairs have non-zero center of mass momentum, and the deformed Fermi surface (DFS) state [12], for which the Fermi surfaces deform to facilitate overlap of the two surfaces.

In this paper, we review our experiments on fermion pairing with ultracold ^{6}Li atoms. In the first experiment, we have used a molecular spectroscopic technique to probe the microscopic physics of pairing near a Feshbach resonance. In the second, we have explored a two spin-component Fermi system in which the populations of the two components are unequal. We have observed phase separation into a fully paired core with the unpaired atoms expelled to the core exterior. The spatial distributions of the two components deform, in violation of spatial isotropy as manifested by the local density approximation (LDA).

2 Apparatus and General Methods

Our methods for producing a degenerate Fermi gas have been discussed in several prior publications [6, 13–15]. Laser-slowed lithium atoms are loaded into a magneto-optical trap, then transferred to a clover-leaf magnetic trap where they are cooled by rf evaporation. Spin symmetry prevents spin-polarized fermions from undergoing s-wave interactions, so in order to thermalize the magnetically-trapped ^{6}Li atoms during evaporation we simultaneously cool and trap ^{7}Li, a boson. The ^{7}Li is directly evaporated, while the ^{6}Li are cooled sympathetically by collisions with the ^{7}Li atoms [13]. Two rf frequencies are used to remove the most energetic ^{6}Li and ^{7}Li atoms [14]. With this dual evaporation technique, the efficiency of evaporation may be maximized by maintaining an equal number of both species. By the end of the evaporation cycle the number of ^{6}Li atoms is greater than 10^7 at a temperature of approximately $0.1T_F$, where T_F is the Fermi temperature. Finally, the remaining ^{7}Li atoms are removed by rf spin flips.

Magnetic trapping of ^{6}Li in the $F = 3/2$, $m_F = 3/2$ state provides long trap lifetimes because of the absence of spin-exchange losses. However, the Feshbach resonance occurs between the $F = 1/2$, $m_F = \pm 1/2$ states, which are not magnetically trappable. Instead, following evaporation an optical trap formed by a focussed infrared laser beam is switched on while the magnetic trap is turned off. Atoms are then transferred to the $F = 1/2$, $m_F = 1/2$ state by an rf sweep. An *incoherent* mixture of the $m_F = \pm 1/2$ states is necessary if the atoms are to interact. The creation of this incoherent mixture is accomplished by a sawtooth succession of frequency ramps through the rf transition coupling the two states. By adjusting the rf power to give an approximately 50% transition probability per sweep, and by passing through the transition 100 times in the presence of an inhomogeneous magnetic field, we obtain an interacting, incoherent mixture of equal populations. The atoms may be further evaporatively cooled in the optical trap by reducing the power of the infrared beam. We typically reduce the trap intensity to approximately 1% of the initial value over a time of about 1 s. At this point, we have a mixture of $N \sim 10^5$ atoms per spin state, and

while the exact temperature T is unknown due to the difficulty in measuring temperatures of highly degenerate Fermi gases, we have determined that $T \lesssim 0.1 T_F$ [6].

3 Results

3.1 Characterization of the Pairs

The BEC-BCS crossover may be realized by tuning the interaction strength via a Feshbach resonance. In a Feshbach resonance, the energy of an atom pair is tuned into resonance with a vibrational level of the diatomic molecule. Generally, a Feshbach resonance involves free atoms interacting via a potential of different symmetry than that supporting the bound vibrational state. In the language of scattering physics, atoms in the "open-channel" interact with a bound state in the "closed-channel". The $F = 1/2, m_F = \pm 1/2$ states of ^{6}Li exhibit a broad Feshbach resonance at 834 G [16, 17]. At this field, these states are very nearly electronically spin-polarized, meaning that the open channel corresponds to a spin-triplet, $S = 1$, where S is the total electronic spin of the two atoms. The closed-channel is an electronic singlet ($S = 0$) state. The hyperfine interaction couples the two channels.

The original proposals for the BEC-BCS crossover came from the condensed matter community [18, 19], where the interaction involved only a single potential. These single-channel models of the crossover exhibit universality, where the properties of the gas depend only on the density, rather than on the details of the microscopic physics of the interaction. There has been considerable discussion in the literature of whether universality survives in a Feshbach resonance, which is inherently a two-channel problem, and whether there are differences between "broad" and "narrow" Feshbach resonances [20–24]. Universality is expected for the broad resonance of ^{6}Li, since the extremely large triplet scattering length of $-2260\, a_o$ [25] (a_o is the Bohr radius) conspires to create an open-channel dominated resonance [26] with a width of well over 100 G [16].

On the BEC side of resonance the pairs are bound and may be described as "dressed molecules", while sufficiently far into the BCS side the pairs are unbound. Throughout the crossover, the dressed molecules/pairs can be expressed as a superposition of the closed channel singlet molecules and free atom pairs in the triplet channel [27]:

$$|\psi_{\mathrm{p}}\rangle = Z^{1/2}|\psi_v(S=0)\rangle + (1-Z)^{1/2}|\phi_{\mathrm{a}}(S=1)\rangle, \tag{1}$$

where Z is the closed-channel component fraction of the pairs.

We used a molecular probe laser to drive transitions between the dressed molecules/pairs and an electronically excited molecular singlet level, $\psi_{v'}(S=0)$. Because of the selection rule $\Delta S = 0$, the optical transition picks out just the singlet component of the pairs. A transition results in spontaneous emission and a detectable loss of molecules/pairs from the trap. The rate of the transition is $\Gamma = Z\Omega^2/\gamma$, where Ω is the on-resonance Rabi frequency, and $\gamma = (2\pi)\ 11.7$ MHz is the linewidth of the excited molecular state [28].

Z is measured at various fields by the following process: first, the molecular gas is prepared at 754 G. The field is then linearly ramped to a new value B and held for

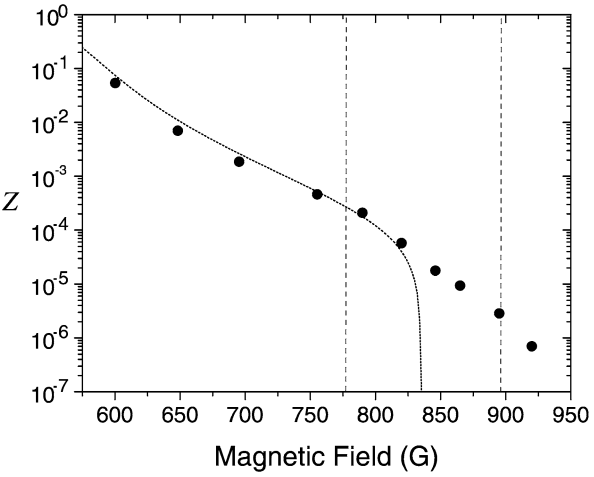

Fig. 1 Z vs. B. The closed circles represent the value of Z extracted from measured values of Γ. The dotted line shows a comparison with results obtained from a coupled channels calculation, assuming two atoms in free space. The vertical dashed lines represent the boundaries of the strongly-interacting regime, $k_F|a| > 1$, where k_F is the Fermi wavevector and is evaluated using typical values of N. The measured values of Z agree well with theory [27, 29, 30]. (Reprinted from [6])

20 ms before the molecular probe is pulsed on for a fixed duration. The probe removes atoms at a rate Γ determined by Z. The field is then linearly returned to 754 G, where the number of remaining atoms is determined by optical absorption imaging. The measured numbers are normalized to data obtained by the same procedure, but without firing the molecular probe. A large dynamic range in Z may be measured by varying the duration of the probe pulse from a few μs to 100's ms.

The results are shown in Fig. 1 for a range of fields between 600 and 920 G. At lower fields, the gas is in the BEC regime, while higher fields correspond to the BCS regime. Most remarkably, the closed-channel fraction is continuous across the Feshbach resonance. The data show no sharp boundaries between the BEC and BCS regimes. In contrast, the dotted line showing the exact two-body result obtained with a coupled-channels calculation reflects the discontinuous nature of the two-body s-wave scattering length, which diverges at the Feshbach resonance.

The closed-channel fraction is $\sim 10^{-5}$ on resonance, meaning that the expectation of the number of closed-channel molecules is less than one. Paradoxically, while the closed-channel creates the Feshbach resonance in the first place, its contribution to the paired state in the strongly interacting regime is almost negligible. This result suggests that a single-channel model might be appropriate to describe the BEC-BCS crossover for this broad resonance. To compare, we note that Γ is proportional to the local pair correlation function $G_2(r,r) = \langle \hat{\psi}_\downarrow^\dagger(r)\hat{\psi}_\uparrow^\dagger(r)\hat{\psi}_\uparrow(r)\hat{\psi}_\downarrow(r)\rangle$, where $\hat{\psi}_\uparrow$ and $\hat{\psi}_\downarrow$ are the fermionic field operators for atoms in different internal states. In the mean-field approximation G_2 may be factorized as $G_2(r,r) = n^2(r) + \langle \hat{\psi}_\downarrow^\dagger(r)\hat{\psi}_\uparrow^\dagger(r)\rangle\langle\hat{\psi}_\uparrow(r)\hat{\psi}_\downarrow(r)\rangle$, where the first term is the Hartree term with atom density $n(r) = n_\uparrow(r) = n_\downarrow(r)$. This term gives rise to a slow two-body photoassociation process that is observed for higher temperatures ($T \simeq 0.75T_F$). The second term is non-zero only for correlated pairs and is proportional to $|\Delta|^2$, the square of the order parameter. $|\Delta|^2$ has been previously evaluated for a single-channel model [31]. In the BCS limit, $|\Delta|^2 \propto \epsilon_F^2 e^{-\pi/(k_F|a|)}$, whereas in the BEC limit, $|\Delta|^2 \propto \epsilon_F^2/(k_F a)$, which is simply proportional to $n(r)$, and produces a rapid one-body loss. In Fig. 2 the data is compared with these functional forms. The fact that the data have the correct

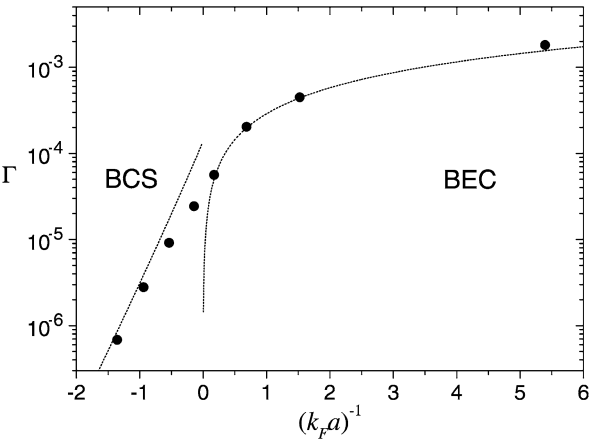

Fig. 2 Comparison of Γ with $|\Delta|^2$. Γ is expressed in units of Ω^2/γ making it equivalent to Z plotted in Fig. 1. The dashed lines correspond to evaluations of $|\Delta|^2$ in the BCS and the BEC limits integrated over a Thomas-Fermi density profile. They have been scaled by the same factor to give the best fit on the BEC side. (Reprinted from [6])

dependence on $(k_F a)^{-1}$ in the BEC and BCS limits suggests that a single-channel model has captured the essential physics. This universality is a consequence of the broad width of this particular Feshbach resonance, which results in $Z \ll 1$. Data obtained by starting with higher initial temperatures do not fit the curves given in Fig. 2.

3.2 Unequal Spin Populations

Unequal numbers of each spin component, N_1 and N_2, can be attained by driving transitions between the $F = 1/2, m_F = \pm 1/2$ states with reduced rf power. Mixtures with polarization P between 0 and 1, where $P = (N_1 - N_2)/(N_1 + N_2)$, are readily created. The mixture is evaporatively cooled by reducing the optical trap intensity, and the real-space atomic distributions of each spin-state are sequentially obtained by in situ imaging [15]. Examples of the resulting images are displayed in Fig. 3. The third image, equal to the difference of the other two, shows the presence of a central hole where the column densities of the two components are nearly equal. The difference, reflecting the distribution of the excess unpaired atoms, reveals a phase separation between an evenly paired core and the unpaired atoms [15]. Phase separation between a superfluid core and a normal fluid has been discussed theoretically [32–36]. Shin et al. have also adopted in-situ imaging, and have recently presented their resulting images as evidence for phase separation [37].

A more detailed examination of the distributions can be obtained by integrating the column density images along the remaining radial coordinate. The resulting axial density distributions for several representative polarizations are displayed in Fig. 4. For $P > P_c$ the axial densities exhibit a characteristic central dip. The central dip is a consequence of the unpaired atoms preferentially residing at the axial poles of the trap, rather than in the equatorial shell, as can be seen in Fig. 3C. It has been shown that the central dip is inconsistent with the combination of harmonic confinement the LDA [38, 39]. In the LDA, all local physics is assumed isotropic, and so the real-space distributions should correspond to the isopotentials of the confining trap. In the experiment, axial confinement is formed mainly by magnetic curvature and to a lesser extent by a focused infrared laser beam, and is harmonic to good approximation. Radial confinement, on the other hand, is produced by the Gaussian waist of the

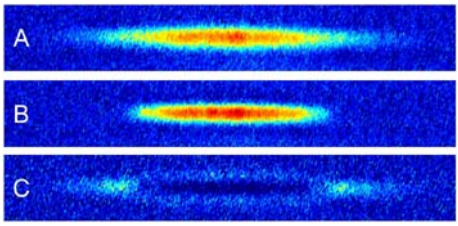

Fig. 3 In situ absorption images showing phase separation at 830 G (color online). These images correspond to $P = 0.14$. **A** Majority spin state, $|1\rangle$, $N_1 = 8.6 \times 10^4$. **B** Minority spin state, $|2\rangle$, with $N_2 = 6.5 \times 10^4$. **C** Difference distribution, $|1\rangle$–$|2\rangle$, corresponding to the excess unpaired $|1\rangle$ atoms. The excess atoms reside outside the inner core of unpolarized pairs, preferentially at the axial poles, while relatively few are observed in the equatorial shell. (Reprinted from [15])

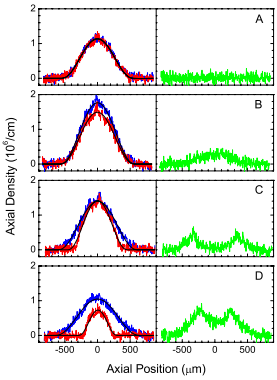

Fig. 4 Axial density profiles at 830 G (color online). Images of each state are shown on the *left*, while the difference distributions are shown on the *right*. The *solid lines* are fits to a Thomas-Fermi distribution for fermions. **A** $P = 0.01$; **B** $P = 0.09$; **C** $P = 0.14$; **D** $P = 0.53$. The minority state distributions reflect the distribution of pairs, while the difference distributions show the unpaired atoms. Phase separation is evident in (**C**) and (**D**). (Reprinted from [15])

laser beam, resulting in an effectively anharmonic potential. Radial anharmonicity causes spreading in the radial direction, primarily for the majority spin component, and hence produces a *peaking* of the axial density profile, and not a dip.

The distributions explicitly violate the LDA. The excess numbers of atoms at the axial poles (Fig. 3) is reflected by a striking variation of the aspect ratio with increasing P. As P is increased, the minority state distribution becomes less elongated and broader radially, enabling the two densities to be nearly equal in the central core. We also observe that the phase boundary between the central core and the unpaired atoms is remarkably sharp, in agreement with expectations for a first-order phase transition.

There have been several mechanisms proposed that may violate the LDA. These mechanisms are enhanced by the high-aspect ratio ($\sim$35) trapping potential employed in our experiment. Surface tension between the normal and superfluid phases can result in deformations of the minority component that are quite similar to those observed here [40]. Also, gradient terms in the Gross-Pitaevskii equation can lead to LDA-violating deformations on the BEC side of resonance, although the magnitude of the calculated effect is much smaller than we observe at unitarity [41]. We obtain

good fits to the data using a model which incorporates surface tension at the phase boundaries and find that there is no evidence for a deformed Fermi surface [42].

We find that the critical polarization, P_c, for the onset of phase separation depends on temperature. Thermometry of low temperature Fermi gases is difficult, although by fitting the column density profiles of gases deliberately prepared as $P = 0$ to fermionic Thomas-Fermi distributions, one can obtain fitted temperatures $\widetilde{T}$ that are expected to be closely related to the actual temperature [5]. For the lowest temperature data, ($\widetilde{T} < 0.05T_F$), the gas phase separates for any non-zero P, corresponding to $P_c = 0$ [42], and the phase boundaries between the superfluid core and the completely polarized normal gas are particularly sharp. For slightly higher temperatures, $\widetilde{T} \simeq 0.1T_F$, we find that $P_c = 0.1$ [15], and that for $P < P_c$, there is no sharp boundary between the core and the normal gas, which is consistent with a polarized superfluid (Sarma) state. At even higher temperatures, $\widetilde{T} \simeq 0.2T_F$, the gas never undergoes a phase separation and there are no deformations, even though there is an evenly paired central core [42]. This temperature dependence suggests that the boundary between the superfluid core and the normal gas at the lowest temperatures is first-order, as expected for a true phase separation, while the boundary at higher temperature is second-order. Such a phase diagram is consistent with the presence of a tricritical point, as was recently proposed [43, 44], where phase separation only occurs for temperatures below the tricritical point. Our higher temperature data, which exhibits an evenly paired core up to finite P but no phase separation, is similar to the data presented in [37] by the MIT group. In their case, the trap aspect ratio is approximately 10 times smaller than ours and surface tension is not expected to produce significant spatial deformations [40].

4 Conclusions

The achievement of Fermi degeneracy with ultracold atoms has lead to the experimental realization of the BEC-BCS crossover. This system is inherently interesting because of the ability to widely tune system parameters, including interactions and the relative numbers of the two spin-states. We have shown that a single-channel model of the crossover is appropriate in the case of the broad ^{6}Li resonance, regaining the concept of universality. We expect that a strongly interacting atomic Fermi gas is completely analogous to strongly interacting Fermi gases encountered elsewhere, including condensed matter systems. Results with unbalanced Fermi gases may also have important implications for our understanding of nuclei, compact stars, and quantum chromodynamics.

Acknowledgements This research is supported by the NSF, ONR, NASA, and the Welch Foundation. We acknowledge many useful discussions with Henk Stoof.

References

1. C.A. Regal, M. Greiner, D.S. Jin, Phys. Rev. Lett. **92**, 040403 (2004)
2. M. Bartenstein et al., Phys. Rev. Lett. **92**, 203201 (2004)
3. M.W. Zwierlein et al., Phys. Rev. Lett. **92**, 120403 (2004)

4. J. Kinast, S.L. Hemmer, M.E. Gehm, A. Turlapov, J.E. Thomas, Phys. Rev. Lett. **92**, 150402 (2004)
5. J. Kinast et al., Science **307**, 1296 (2005)
6. G.B. Partridge, K.E. Strecker, R.I. Kamar, M.W. Jack, R.G. Hulet, Phys. Rev. Lett. **95**, 020404 (2005)
7. M.W. Zwierlein, J.R. Abo-Shaeer, A. Schirotzek, C.H. Schunck, W. Ketterle, Nature **435**, 1047 (2005)
8. R.A. Duine, H.T.C. Stoof, Phys. Rep. **396**, 115 (2004)
9. G. Sarma, J. Phys. Chem. Solids **24**, 1029 (1963)
10. P. Fulde, R.A. Ferrell, Phys. Rev. **135**, A550 (1964)
11. J. Larkin, Y.N. Ovchinnikov, Sov. Phys. J. Exp. Theor. Phys. **20**, 762 (1965)
12. A. Sedrakian, J. Mur-Petit, A. Polls, H. Müther, Phys. Rev. A **72**, 013613 (2005)
13. A.G. Truscott, K.E. Strecker, W.I. McAlexander, G.B. Partridge, R.G. Hulet, Science **291**, 2570 (2001)
14. K.E. Strecker, G.B. Partridge, R.G. Hulet, Phys. Rev. Lett. **91**, 080406 (2003)
15. G.B. Partridge, W. Li, R.I. Kamar, Y.A. Liao, R.G. Hulet, Science **311**, 503 (2006)
16. M. Houbiers, H.T.C. Stoof, W.I. McAlexander, R.G. Hulet, Phys. Rev. A **57**, R1497 (1998)
17. M. Bartenstein et al., Phys. Rev. Lett. **94**, 103201 (2005)
18. A.J. Leggett, *Modern Trends in the Theory of Condensed Matter* (Springer, Berlin, 1980)
19. P. Nozières, S. Schmitt-Rink, J. Low Temp. Phys. **59** (1985)
20. R. Combescot, Phys. Rev. Lett. **91**, 120401 (2003)
21. G.M. Bruun, Phys. Rev. A **70**, 053602 (2004)
22. S. De Palo, M.L. Chiofalo, M.J. Holland, S.J.J.M.F. Kokkelmans, Phys. Lett. A **327**, 490 (2004)
23. S. Simonucci, P. Pieri, G.C. Strinati, Europhys. Lett. **69**, 713 (2005)
24. M. Szymaska, K. Góral, T. Köhler, K. Burnett, Phys. Rev. A **72**, 013610 (2005)
25. E.R.I. Abraham et al., Phys. Rev. A **55**, R3299 (1997)
26. B. Marcelis, E.G.M. van Kempen, B.J. Verhaar, S.J.J.M.F. Kokkelmans, Phys. Rev. A **70**, 012701 (2004)
27. M.W.J. Romans, H.T.C. Stoof, Phys. Rev. Lett. **95**, 260407 (2005)
28. I.D. Prodan, M. Pichler, M. Junker, R.G. Hulet, J.L. Bohn, Phys. Rev. Lett. **91**, 080402 (2003)
29. J. Javanainen, M. Koštrun, C. Mackie, A. Carmichael, Phys. Rev. Lett. **95**, 110408 (2005)
30. Q. Chen, K. Levin, Phys. Rev. Lett. **95**, 260406 (2006)
31. J.R. Engelbrecht, M. Randeria, C.A.R. Sá de Melo, Phys. Rev. B **55**, 15153 (1997)
32. P.F. Bedaque, H. Caldas, G. Rupak, Phys. Rev. Lett. **91**, 247002 (2003)
33. J. Carlson, S. Reddy, Phys. Rev. Lett. **95**, 060401 (2005)
34. D.E. Sheehy, L. Radzihovsky, Phys. Rev. Lett. **96**, 060401 (2006)
35. Z.-C. Gu, G. Warner, F. Zhou, cond-mat/0603091 (2006)
36. H. Hu, X.-J. Liu, Phys. Rev. A **73**, 051603 (2006)
37. Y. Shin, M.W. Zwierlein, C.H. Schunck, A. Schirotzek, W. Ketterle, Phys. Rev. Lett. **97**, 030401 (2006)
38. T.N. De Silva, E.J. Mueller, Phys. Rev. A **73**, 051602 (2006)
39. M. Haque, H.T.C. Stoof, Phys. Rev. A **74**, 011602(R) (2006)
40. T.N. De Silva, E.J. Mueller, Phys. Rev. Lett. **97**, 070402 (2006)
41. A. Imambekov, C.J. Bolech, M. Lukin, E. Demler, Phys. Rev. A **74**, 053626 (2006)
42. G.B. Partridge et al., Phys. Rev. Lett. **97**, 190407 (2006)
43. M.M. Parish, F.M. Marchetti, A. Lamacraft, B.D. Simons, Nat. Phys. **3**, 124 (2007)
44. K.B. Gubbels, M.W.J. Romans, H.T.C. Stoof, Phys. Rev. Lett. **97**, 210402 (2006)